# Folding of poly-amino acids and intrinsically disordered proteins in overcrowded milieu induced by pH change

Fonin, Alexander V.

2019-03-15

Fonin , A V , Stepanenko , O V , Sitdikova , A K , Antifeeva , I A , Kostyleva , E I , Polyanichko , A M , Karasev , M M , Silonov , S A , Povarova , O I , Kuznetsova , I M , Uversky , V N & Turoverov , K K 2019 , ' Folding of poly-amino acids and intrinsically disordered proteins in overcrowded milieu induced by pH change ' , International Journal of Biological Macromolecules , vol. 125 , pp. 244-255 . https://doi.org/10.1016/j.ijbiomac.2018.12.038

http://hdl.handle.net/10138/312558
https://doi.org/10.1016/j.ijbiomac.2018.12.038

unspecified
publishedVersion

International Journal of Biological Macromolecules 125 (2019) 244–255

Contents lists available at ScienceDirect

International Journal of Biological Macromolecules

journal homepage: http://www.elsevier.com/locate/ijbiomac

# Folding of poly-amino acids and intrinsically disordered proteins in overcrowded milieu induced by pH change

Alexander V. Fonin [a], Olga V. Stepanenko [a], Asiia K. Sitdikova [a], Iuliia A. Antifeeva [a], Elena I. Kostyleva [a], Alexander M. Polyanichko [b], Maksim M. Karasev [c], Sergey A. Silonov [a], Olga I. Povarova [a], Irina M. Kuznetsova [a], Vladimir N. Uversky [d,*], Konstantin K. Turoverov [a,e,**]

[a] Institute of Cytology of the Russian Academy of Sciences, Laboratory of Structural Dynamics, Stability and Folding of Proteins, Tikhoretsky av. 4, St. Petersburg, Russia
[b] Saint-Petersburg State University, Physical Faculty, Universitetskaya nab., 7-9, St. Petersburg, Russia
[c] University of Helsinki, Faculty of Medicine, Haartmaninkatu 8, Helsinki, Finland
[d] University of South Florida, Morsani College of Medicine, Department of Molecular Medicine and Byrd Alzheimer's Research Institute, FL 33612, Tampa, USA
[e] Peter the Great St. Petersburg Polytechnic University, Department of Biophysics, Polytechnicheskaya av. 29, St. Petersburg, Russia

ARTICLE INFO

*Article history:*
Received 9 October 2018
Received in revised form 27 November 2018
Accepted 2 December 2018
Available online 5 December 2018

ABSTRACT

pH-induced structural changes of the synthetic homopolypeptides poly-E, poly-K, poly-R, and intrinsically disordered proteins (IDPs) prothymosin α (ProTα) and linker histone H1, in concentrated PEG solutions simulating macromolecular crowding conditions within the membrane-less organelles, were characterized. The conformational transitions of the studied poly-amino acids in the concentrated PEG solutions depend on the polymerization degree of these homopolypeptides, the size of their side chains, the charge distribution of the side chains, and the crowding agent concentration. The results obtained for poly-amino acids are valid for IDPs having a significant total charge. The overcrowded conditions promote a significant increase in the cooperativity of the pH-induced coil–α-helix transition of ProTα and provoke histone H1 aggregation. The most favorable conditions for the pH-induced structural transitions in concentrated PEG solutions are realized when the charged residues are grouped in blocks, and when the distance between the end of the side group carrying charge and the backbone is small. Therefore, the block-wise distribution of charged residues within the IDPs not only plays an important role in the liquid–liquid phase transitions, but may also define the expressivity of structural transitions of these proteins in the overcrowded conditions of the membrane-less organelles.



## 1. Introduction

Liquid–liquid phase transitions (LLPTs) of intrinsically disordered proteins (IDPs) and hybrid proteins containing ordered domains and intrinsically disordered regions (IDPRs) under the conditions of macromolecular crowding have a vital role in cellular life [1–3]. The conditions for phase separation of such proteins in a cell are created at high concentrations of macromolecules, and are regulated by different cellular signals [1,4–7]. These processes are the basis for the formation of the proteinaceous membrane-less organelles (PMLOs), which are highly dynamic structures that are able to form for solving definite tasks, and rapidly disintegrate after these tasks have been completed [8–13]. The decisive role of IDPRs and IDPs in the formation of the PMLOs is defined by the presence of blocks of polar, charged, and aromatic residues in the sequences of these proteins. However, it should also be noted that not all IDPs/IDPRs involved in phase separation leading to the PMLO formation have "blocks" of these residue types, and there is a large variety of sequence characteristics that can support phase separation. Under the conditions of limited free volume, the weak intermolecular electrostatic or stacking interactions between these charged and aromatic residues and the multivalence of IDPs/IDPRs regulate the LLPT transitions of IDPRs and IDPs into the liquid droplet phase [5,8,13–17]. The changes in the electrostatic characteristics of such proteins/regions induced by the medium pH changes or due to the posttranslational modifications may have a significant effect on the assembly/disassembly, composition, structure, and functioning of various PMLOs [8,9,18].

The absence of strictly deterministic structure allows IDPs/IDPRs to have a wide range of conformational states, with the transition between these states being caused by various factors, such as changes in the polypeptide chain charge [19–47]. The changes in the protein conformation can determine its ability to interact with various partners, as well as

* Corresponding author.
** Correspondence to: K.K. Turoverov, Institute of Cytology of the Russian Academy of Sciences, Laboratory of Structural Dynamics, Stability and Folding of Proteins, Tikhoretsky av. 4, St. Petersburg, Russia.
*E-mail addresses:* vuversky@health.usf.edu (V.N. Uversky), kkt@incras.ru (K.K Turoverov).

https://doi.org/10.1016/j.ijbiomac.2018.12.038
0141-8130/

change the threshold concentration required for protein transition into the liquid droplet phase, or induce protein aggregation.

Intracellular space is marked by a minimal free water content and the presence of continual steric contacts between the macromolecules (macromolecular crowding conditions). However, proteins included into the PMLOs function under the overcrowded conditions created by the presence of ultrahigh concentrations of other biopolymers [19]. Such conditions can significantly affect the structure and functional activity of proteins [32,48–56].

At present, substantial information has been accumulated pertaining to the effect of macromolecular crowding on IDPs structure [57]. It was established that, based on the peculiarities of the action of macromolecular crowding conditions on the structure of these proteins, many IDPs can be divided into three groups: foldable (i.e., IDPs/IDPRs undergoing crowding-induced (partial) folding), non-foldable (i.e., IDPs/IDPRs that remain mostly disordered in crowded environments), and unfoldable (i.e., IDPs/IDPRs that are characterized by crowding-induced (partial) unfolding of their residual structure) [57]. However, one should also keep in mind that such classification represents an oversimplification, since not all IDPs can be classified into these three groups, as there are too many possibilities in-between these groups, and there are even cases that do not fit into this classification. At the same time, the details of conformational changes of IDPs provoked by the macromolecular crowding conditions remain practically unexplored. According to modern concepts, IDPs are open dynamic systems that exist at the edge of chaos, and whose evolution and functionality critically depends on the external environment and initial conditions [58–60]. This suggests that macromolecular crowding might have different effects on the conformational changes of different IDPs.

Understanding the mechanisms of different conformational transitions in different IDPs caused by macromolecular crowding in vitro will help determine the molecular principles that underlie the conformational changes of IDPs/IDPRs in the intracellular space, including structural reorganizations taking place within the PMLOs. Typically, the conditions of macromolecular crowding in intracellular space are modeled in vitro by utilizing highly concentrated solutions of "inert" polymers, such as polyethylene glycol (PEG), Dextran, or Ficoll. In order to simulate overcrowding conditions that are characteristic for a protein environment inside the PMLOs, in this study we used PEG solutions with molecular masses ranging from 600 to 12,000 Da, in concentrations ranging from 80 to 300 mg/mL. In such solutions, there is almost no free space unoccupied by the crowding agent molecules (Fig. S1). Therefore, under such conditions, PEG is essentially a hydrogel and forms cluster structures due to the hydrophobic interactions between polymer chains of the crowding agent [61–63].

Conformational transitions in IDPs with large net charge can be approximated by conformational transitions of homopolypeptides of charged amino acids. This is possible because, firstly, poly-amino acids do not have an ordered spatial structure, similar to extended IDPs. Secondly, the charged residues of IDPs engaged in the PMLO formation are in certain cases grouped in blocks, and are not evenly distributed within the protein amino acid sequence.

In the present work, we analyzed the pH-induced conformational changes in poly-L-glutamic acid (poly-E), poly-L-lysine (poly-K), and poly-L-arginine (poly-R) in concentrated solutions of PEG of various molecular weights. This analysis revealed that, due to the electrostatic repulsion between their like-charged groups, poly-K and poly-R at acidic and neutral pH, and poly-E at alkaline and neutral pH, have an unordered structure. However, the decrease in the electrostatic repulsion between the charged groups of polypeptides, when solution pH is shifted to the alkaline region (in the case of poly-K and poly-R) or to the acidic region (in the case of poly-E), causes the formation of α-helical structure by these poly-amino acids [64–69]. Poly-K and poly-E can be considered as models of extended IDPs, linker histone H1 and prothymosin α (ProTα), whose amino acid sequences contain respectively ~30% of lysine and glutamic acid residues. Therefore, in addition to the analysis of the effect of high PEG concentrations on pH-induced conformational changes in the aforementioned homopolypeptides, we characterized the pH-induced conformational transitions in ProTα and H1 histone proteins at the conditions of macromolecular crowding.

## 2. Materials and methods

### 2.1. Materials

PEG 600, PEG 4000, PEG 12,000, KCl, HCl, citric acid, $Na_2HPO_4$, $NaH_2PO_4$, $Na_2B_4O_7$, glycine, NaOH (Sigma, USA), poly-K, poly-E, and poly-R (Alamanda Polymers, USA) were used without further purification. Solutions used in this study were based on the Clark-Lubs, citric acid-sodium phosphate, sodium phosphate, glycine, borate, NaOH-KCl buffers, with pH ranging from 2 to 12. To determine the pH of tested solutions, we used the HI-9024 pH-meter equipped with the FC-200 electrode for viscous medium (HANNA Instruments, USA).

### 2.2. Linker histone H1 purification

Linker histone H1 (MW 21,000 Da) was purified from calf thymus chromatin by extraction with 5% perchloric acid with subsequent precipitation of the proteins from the solution with acidic acetone at −20 °C as described earlier [70,71]. The identification of protein and its purity were tested by SDS-PAGE as described elsewhere [72]. The purified protein was stored in the lyophilized form. For the spectroscopic experiments, the dry protein samples were dissolved in aqueous solutions. The exact concentration of linker histone H1 in the tested solutions was determined spectrophotometrically using the molar extinction coefficient of $\varepsilon_{230} = 41{,}000\ M^{-1}\ cm^{-1}$.

### 2.3. Production and purification of the recombinant prothymosin α

Recombinant prothymosin α (ProTα) was obtained via expression in the *E. coli* BL21 (DE3) cells. The use of the cytoplasmic expression of ProTα resulted in the extremely low yields of this protein in cell lysate. This may be caused by the toxicity of ProTα for bacterial cells and/or by the susceptibility of this protein to bacterial proteases due to its highly disordered nature. To increase the target protein yield, a construct that carries the gene encoding ProTα linked to the PelB leader sequence was created. The PelB sequence directs the protein product containing it in the bacterial cell periplasm. This decreases the concentration of a target protein in the bacterial cytoplasm, and also protects it from the action of proteases. The PelB leader sequence is deleted in the periplasm due to the action of the signal peptidase. At the same time, ProTα gradually "flows" into the culture medium, likely as a result of changes in the permeability of the cell outer membrane due to intensive mixing of the bacterial culture during protein expression, as well as due to the high negative charge of ProTα.

The cells transformed with the developed construct were spread on a Petri dish with low salt LB medium (10 g/L tryptone, 5 g/L yeast extract, 5 g/L NaCl, 15 g/L agar, pH 7.5) containing 100 μg/mL ampicillin. The resulting dish was incubated overnight at 37 °C. Then, a single colony from the plate was transferred into 8 mL of fresh low-salt LB medium containing 100 μg/mL ampicillin, followed by the overnight incubation at 37 °C with stirring. After 12 h, the resulting culture was inoculated into 200 mL of TB medium (12 g/L tryptone, 24 g/L yeast extract, 4% glycerol, 2.2 g/L $KH_2PO_4$, 9.4 g/L $K_2HPO_4$) containing 100 μg/mL ampicillin and incubated at 37 °C with stirring (250 rpm) until reaching $A_{600}$ ~ 0.8–1. The protein expression was induced by the addition of 0.02 mM IPTG. The resulting sample was kept overnight at 37 °C with intense stirring (250 rpm). The bacterial cells were removed from the culture medium by centrifugation (5000 rpm, 30 min) on the next morning. Then, DTT was introduced into the supernatant to the final concentration of 1 mM. The resulting solution was incubated in 100 °C water bath for 20 min, after which it was transferred to −10 °C for

1 h. The resulting precipitate was removed by centrifugation (9500 rpm, 1 h). Next, protein purification was carried out according to the method described in [73]. The purity of the sample was controlled by the SDS-PAGE. The yield of protein from the 200 mL of medium was 13.6 mg.

### 2.4. Circular dichroism measurements

CD spectra were obtained using Jasco-810 spectropolarimeter (Jasco, Japan). Far-UV CD spectra were recorded in a 1 mm path-length cell from 260 nm to 190 nm with a step size of 0.1 nm. For all spectra, an average of 3 scans was obtained. CD spectra of the appropriate buffer solution were recorded and subtracted from the sample CD spectra. Analysis of the distribution of elements in the secondary structure of the studied samples according to the CD data was performed using the package CDpro [74].

The proportion of α-helixes in the poly-amino acids structure was estimated according to

$$f_H = \frac{\theta - \theta_{coil}}{\theta_{helix} - \theta_{coil}} \quad (1)$$

where $\theta$ is molar ellipticity, $\theta_{coil}$ is molar ellipticity corresponding to poly-amino acids with disordered structure, and $\theta_{helix}$ is molar ellipticity equal to 37,000 $cm^2\ mol^{-1}$ corresponding to a polypeptide containing 100% α-helixes [75,76].

The cooperativity of the coil–helix transition was estimated by the $\sigma$ parameter, which is used in the Zimm-Bragg model [77]. According to [78], the proportion of α-helixes in the structure of poly-amino acids can be represented as

$$f_H = \frac{1}{2} + \frac{(s-1)}{2\sqrt{(s-1)^2 + 4\sigma s}} \quad (2)$$

where $s = e^{-\frac{\Delta F_0}{RT}}$, $\sigma = e^{-\frac{\Delta F_{in}}{RT}}$, and $\Delta F_0$ is the change in the Hemholtz free energy when the α-helix region of polypeptide chain is lengthened by one monomer unit, whereas $\Delta F_{in}$ is the change in the Hemholtz free energy associated with the initiation of α-helical structure formation [79].

Taking into account that in the close proximity to the middle of transition between disordered and α-helical form of a polypeptide [80]

$$\Delta F_0 = \frac{\Delta pH}{0.434RT}, \quad (3)$$

we can write the following expression:

$$\left(\frac{df_H}{dpH}\right)_{f_H=0.5} = \left(\frac{df_H}{ds}\right)\left(\frac{ds}{dpH}\right)_{pH=pH*} = -\frac{1}{4\sqrt{\sigma}}\frac{1}{0.434} \quad (4)$$

and use it to determine the parameter $\sigma$.

### 2.5. Infrared spectroscopy measurements

The samples of the polypeptides for IR measurements were prepared in $D_2O$ solutions. The mid-IR absorption spectra of the polypeptides in $D_2O$ were obtained with a Fourier-spectrometer Tensor 27 (Bruker, Germany) using a demountable cell with $CaF_2$ windows and 50 μm Teflon spacer. Spectra were recorded by two sequential measurements of 300 accumulations, each with a resolution of 2 $cm^{-1}$ in the range of 4000–900 $cm^{-1}$. The optic pathways of the instrument were purged with gaseous nitrogen. The spectra were registered using a low-noise MCT-detector (HgCdTe) cooled with liquid nitrogen. The analysis of the polypeptide secondary structure was performed as described elsewhere [81–84].

### 2.6. Evaluation of the intrinsic disorder predisposition of linker histone H1 and ProTα

Intrinsic disorder predisposition of bovine linker histone H1 (UniProt ID: P02253) and bovine ProTα (UniProt ID: P01252) were evaluated using several commonly utilized disorder predictors, such as PONDR® VLXT [85], PONDR® VSL2 [86], PONDR® VL3 [86,87], PONDR® FIT [88], IUPred_short, and IUPred_long [89,90]. Justification for the selection of these tools is provided in our previous publications [91,92]. We also generated a mean per-residue intrinsic disorder profile for a given protein by averaging the outputs of these six per-residue disorder predictors, and this mean disorder profile was also added to the corresponding plot. Use of consensus for evaluation of intrinsic disorder is motivated by empirical observations that this approach usually increases the predictive performance compared to the use of a single predictor [93–95]. The outputs of the evaluation of the per-residue disorder propensity by these tools are represented as the real numbers between 1 (ideal prediction of disorder) and 0 (ideal prediction of order). A threshold of ≥0.5 was used to identify disordered residues and regions in query proteins, whereas residues/regions characterized by the disorder scores ranging from 0.2 to 0.5 are classified as flexible.

### 2.7. Charge-based analysis of intrinsic disorder status of linker histone H1 and ProTα

We used the CIDER v1.7 platform (http://pappulab.wustl.edu/CIDER/analysis/) to classify intrinsic disorder predisposition of studied proteins based on their charge content [96]. CIDER provides several useful outputs, including a Das-Pappu phase diagram that represents a means to estimate potential conformational behavior of a query protein based on its charge content, and also shows peculiarities of the charged residues distribution within the query sequence in the form of a linear net charge per residue diagram, which is calculated using a sliding, overlapping window approach to compute the net charge for groups of 5 residues [96].

## 3. Results and discussion

### 3.1. Conformational changes of poly-E and poly-K in diluted solutions

The characteristics of coil–α-helix transitions in poly-amino acids are determined by polymerization degree of the polypeptides and properties of their side groups [97]. To identify the effect of these factors on the coil–α-helix transitions in poly-lysine and poly-glutamic acid in the absence of crowding agents, the pH-induced structural changes of these homopolypeptides with different polymerization degree were characterized. The size of the side group determines the conformational space, which is available for the main chain. Consequently, the ability of poly-amino acids with the same degree of polymerization to form α-helix increases as the size of the side group increases. In the limiting case of poly-glycine, α-helix is not formed [98]. Therefore, as could be expected, in the aqueous solution (in the absence of crowding agents) the ability to form α-helix for poly-K was higher than for poly-E (Fig. 1).

An increase in the polymerization degree of poly-E and poly-K resulted in an increase in the cooperativity of the pH-induced conformational transitions of these poly-amino acids from the disordered to α-helical form (Fig. 1), which is consistent with literature data [75]. This effect is due to the fact that the helix formation by lengthened regions of the polypeptide chain is energetically more favorable than the formation of ordered structure by separate short chain fragments [75]. This result is based on two factors: first, the initiation of α-helical structure formation is associated with the need to fix three amino acid residues (and, accordingly, six dihedral angles) during the formation of the first hydrogen bond. Second, elongation of the α-helix requires the fixation of only one amino acid residue, and therefore this helix elongation process is not as entropy costly as helix initiation. Furthermore, a significant

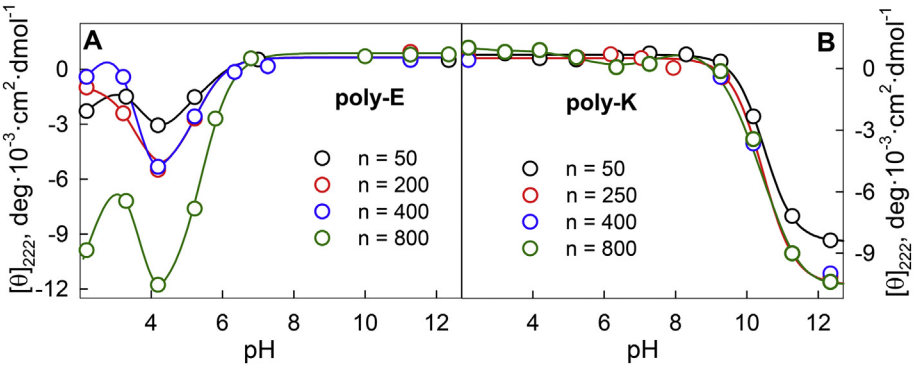


**Fig. 1.** pH-induced conformational changes of poly-E (panel A) and poly-K (panel B) with different polymerization degree in solutions without PEG. The dependences of the molar ellipticity at 222 nm of poly-K and poly-E with the polymerization degrees of 50, 250 (200 for poly-E), 400 and 800 on pH are represented by black, blue, green, and red curves, respectively.

contribution to the decrease in the free energy associated with the α-helix formation is determined by the enthalpy decrease due to the dipole–dipole interactions between the amino groups of the non-adjacent residues [99], with the energy of these dipole–dipole interactions reaching saturation at a certain length of the α-helix [99].

The experimental data obtained in this study correlated strongly with the literature data on the increase of cooperativity of the coil–α-helix transition on the polymerization degree of a polypeptide chain. For poly-E, the cooperativity of coil–α-helix transition increases throughout the whole range of studied molecular weights, from $n = 50$ to $n = 800$; the cooperativity of poly-K conformational transformations increases with the increase of $n$ from 50 to 250, and does not depend on the degree of polymerization when $n$ changes from 250 to 800. Also, our experimental data for poly-E suggest that in the region of acid pH, there are two processes, one of which is associated with the deionization of the carboxyl group of the side chains of glutamic acid and leads to the formation of the α-helix, whereas in the region of pH < 3, the high concentrations of $H^+$ ions could prevent (impede) formation of hydrogen bonds formation between C═O and NH groups of the main chain. Apparently, in this pH region, the poly-E forms disordered globules, as shown by Tran et al. for poly-glycine [98], and aggregate.

pH-induced conformational changes in the poly-E and poly-K in concentrated PEG solutions.

In order to evaluate the effect of conditions of macromolecular crowding on the conformational changes of the studied poly-amino acids, the pH-induced structural transitions in poly-E and poly-K were studied in solutions of PEG with different molecular weights and concentrations.

### *3.2. pH-induced conformational changes in the poly-E in the presence of PEG*

An increase in the PEG content had practically no effect on the midpoint of the pH-induced transition from the disordered to structured form of the poly-E for all PEGs analyzed in this study (Fig. 2). However, the increase in the cooperativity of coil–α-helix transition with PEG concentration growth was observed irrespective of the molecular mass of this crowding agent.

It should be kept in mind that PEGs that are used to mimic macromolecular crowding conditions can form hydrogen bonds [100,101]. When switching from neutral to acidic pH in the presence of PEG, on the one hand, the interaction of PEG with $H^+$ can prevent the neutralization of glutamic acid, but on the other hand, due to the excluded volume effects [31,33,51], it can promote the initiation of α-helices. The interplay between these two oppositely directed effects leads to a significant increase in the cooperativity of coil–α-helix transition (Figs. 2 and 3). The increase in the PEG concentration results in an increase in the cooperativity of transition and increase in the α-helices content. A further increase in the content of $H^+$ ions, which led to the destruction of the α-helix in aqueous solutions, is not observed in PEG solutions. This is apparently also due to the ability of PEG to form hydrogen bonds.

It should be noted that in poly-E solutions with low polymerization degree, the conditions of macromolecular crowding lead to the significant increase in the transition cooperativity. In poly-E with a high polymerization degree, compaction of a polypeptide chain under the conditions of limited free volume no longer caused a significant increase in the transition cooperativity of polypeptide chain (Fig.4). This is likely caused by the length and number of α-helical regions of poly-E with high polymerization degree close to the critical length of helical regions for this poly-amino acid.

### *3.3. pH-induced conformational changes in the poly-K in concentrated PEG solutions*

Our analysis revealed that regardless of the PEG molecular weight, an increase in the concentration of this crowding agent significantly reduced the cooperativity of the structural transition and shifted the transition between the disordered and structured forms of poly-K to a more acidic pH region (Figs. 2–4). This process was further complicated by the poly-K aggregation (Fig. S2). These data indicated that under the conditions of macromolecular crowding, poly-K is able to form an ordered structure much easier compared to the dilute solutions (deprotonation of the ε-amino groups of lysine occurred within the more acidic pH range). Interestingly, at acidic pH, the excluded volume effect of PEG and the hydrogen bonds it forms [100,101] act in different directions, which leads to an increase in the transition cooperativity with the increase in the PEG concentration at alkaline pH; the same effects are summed up and lead to a decrease in the cooperativity of the coil–α-helix transition with increasing PEG concentration.

Also, when changing the solution pH under the conditions of macromolecular crowding, the poly-K polypeptide chains with relatively high polymerization degree are more prone to form new α-helices and aggregate than lengthen the existing α-helical regions (Fig. 4). Similar effects were observed when studying the temperature-induced conformational transitions in poly-E under the conditions of limited free volume [102].

### *3.4. Effects of side chain groups on the pH-induced conformational transitions in the poly-amino acids in crowded milieu*

In order to obtain a more complete picture of the effect of a side chain group on the structural changes of the poly-amino acids under the conditions of macromolecular crowding, conformational changes of poly-arginine with the polymerization degree of 100 were studied in highly concentrated PEG solutions. The chemical structure of the

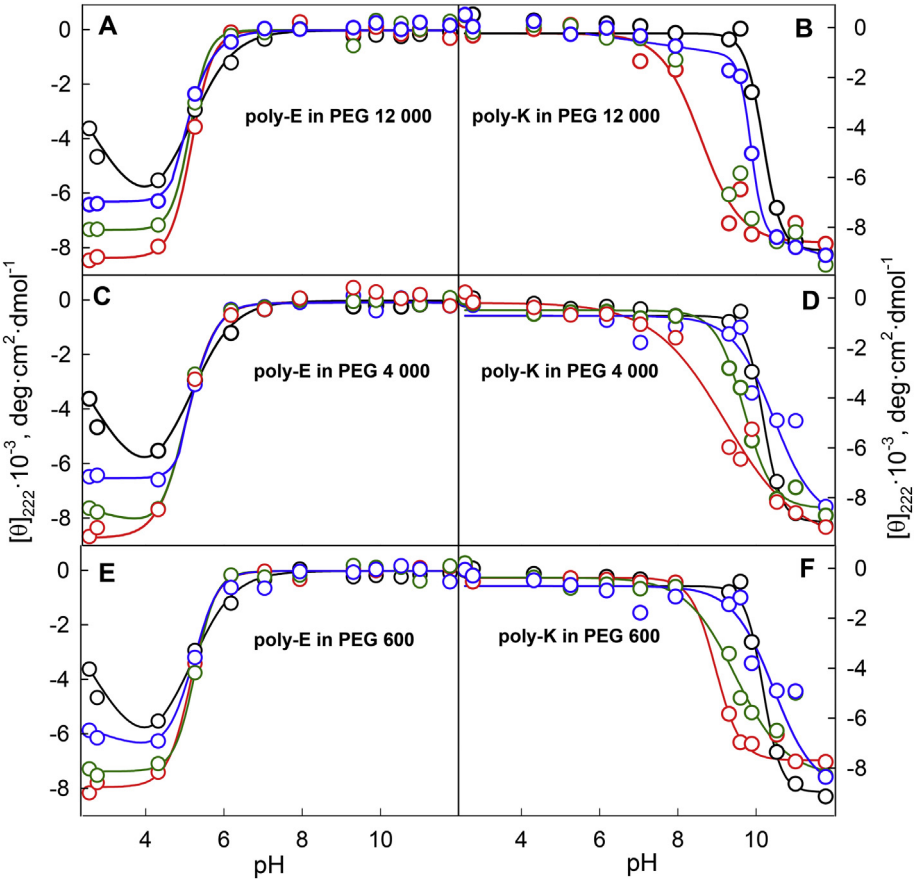


**Fig. 2.** pH-induced conformational changes of poly-E (panels A, C, D) and poly-K (panels B, D, F) in PEG 12,000 (panels A, B), PEG 4000 (panels C, D) and PEG 600 (panels E, F) solutions. The polymerization degree of poly-amino acids was 200 (for poly-E) and 250 (for poly-K). The dependences of molar ellipticity at 222 nm of poly-K and poly-E in PEG solutions with polymer concentrations of 0, 80, 200, and 300 mg/mL on pH are represented by black, blue, green, and red curves, respectively.

arginine side chain ($C_4H_{11}N_3$) is not too different from the chemical structure of the lysine side group ($C_4H_{11}N$), but unlike poly-K, the positive charge of the side chain of poly-R is delocalized. Similar to poly-K, poly-R has a disordered structure at acidic and neutral pH.

However, Arg is characterized by a very high pKa (pH 12.48), which results from the delocalization of the positive charge within the π-bonded system of the side chain guanidinium ion. The guanidinium is so stable that the Arg side chain remains protonated even when partially buried within the protein structure. Furthermore, a protonated guanidinium ion is predominantly solvated in its molecular plane [103]. This could affect the properties of five possible hydrogen bonds, which are formed by the guanidinium group. Contrary to Arg, the Lys charge is radially distributed and is largely focused on the terminal aliphatic amino group, and the side chain is readily deprotonated in proteins [104]. Also, the Lys radical could form only three hydrogen bonds. This may be the reason for the significant differences in the dependencies registered for poly-K and poly-R.

It was established that under the conditions of macromolecular crowding, changes in the solution pH caused the poly-R aggregation, rather than the ordering of this homopolypeptide (Fig. 5). This may occur due to the existence of the resonant structures of guanidine group and its ability to form multiple hydrogen bonds with solvent.

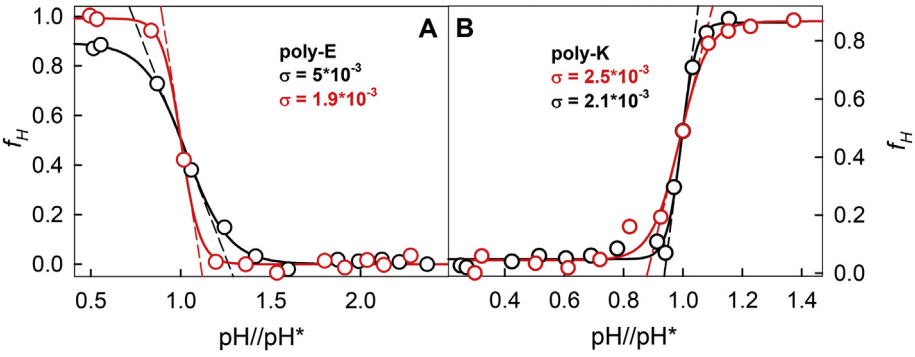


**Fig. 3.** The pH dependences of the content of α-helical regions in the of poly-E (panel A) and poly-K (panel B) structures in the solutions without PEG and in solutions containing 300 mg/mL of PEG 12,000 are represented by black and red curves, respectively. The polymerization degree of poly-amino acids was 200 (for poly-E) and 250 (for poly-K). For convenience of presenting cooperativity of poly-amino acids transition, the abscissa scale is expressed in coordinates pH/pH*, where pH* is the pH value at which the proportion of α-helical regions in the structure of the studied polypeptides is 0.5.

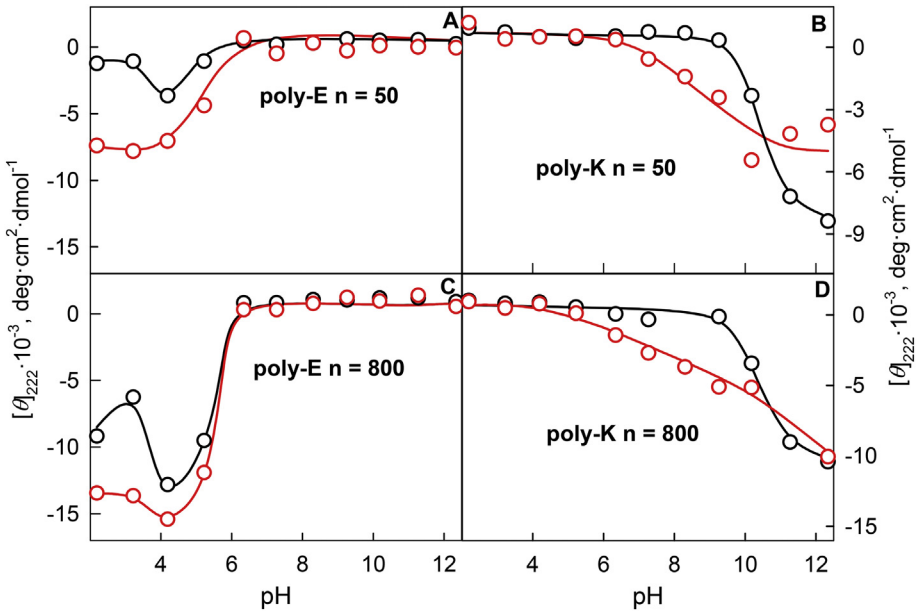


**Fig. 4.** The pH dependences of the molar ellipticity at 222 nm of poly-E (panels A, C) and poly-K (B, D) in the absence of PEG and in solutions containing 300 mg/mL of PEG 12,000 are represented by black and red curves, respectively. The polymerization degree of the poly-amino acids was 50 (panels A, B) and 800 (panels C, D).

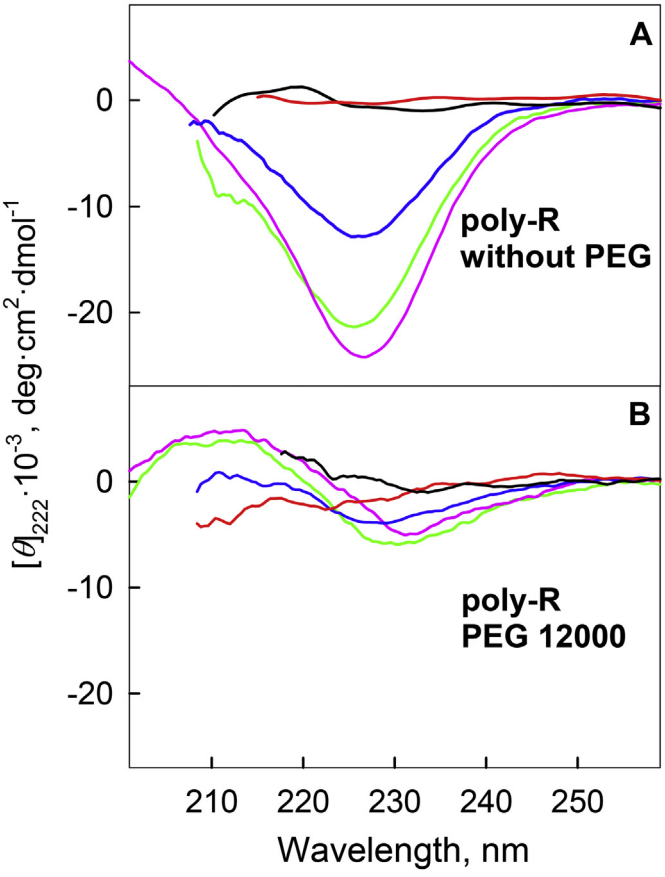


**Fig. 5.** pH-induced conformational changes of poly-R in the absence of PEG (panel A) and in the presence of 300 mg/mL of PEG 12,000 (panel B). The polymerization degree of poly-R was 100. The CD spectra of poly-R in solutions with pH 2.76, 6.18, 6.96, 11.01, and 11.78 are represented by black, red, blue, pink, and green curves, respectively.

The obtained results testify that, based on their ability to aggregate under the macromolecular crowding conditions, the homopolypeptides analyzed in this study can be arranged in the following order: poly-E → poly-K → poly-R. This ordering can be related to the degree of the lability and charge distribution of their side groups.

The obtained data allow us to conclude that the free energy of the coil–α-helix transitions in the studied poly-amino acids were apparently determined by the polymerization degree of the polypeptide and the properties of their side chains. It should be noted that the molecular mass of crowding agents used in the experiment had practically no effect on the conformational transitions of the poly-amino acids analyzed in this study. This may be due to the almost complete absence of free volume in the studied solutions [102].

### *3.5. Intrinsic disorder status and peculiarities of charge distribution in the amino acid sequences of ProTα and linker histone H1*

To understand how intrinsic disorder predisposition is encoded in the amino acid sequences of the bovine linker histone H1 and ProTα, we utilized a set of per-residue disorder predictors of the PONDR family, such as PONDR® VLXT, PONDR® VL3, PONDR® VSL2, and PONDR® FIT. Access to these computational tools was provided by the DisProt database (http://original.disprot.org/) [105,106]. We also used IUPred platform [89] to evaluate the predisposition of these proteins to have short and long intrinsically disordered regions. Results of these analyses are presented in Fig. 6. In line with previous reports [107–112], this multiparametric analysis revealed that both proteins are characterized by very high intrinsic disorder content. It should be noted that histone H1 is not a "pure" IDP; rather it can be referred to as a hybrid protein containing ordered domain and IDPRs. In fact, Fig. 6A shows that this protein contains the central more ordered domain (residues 50–120) and highly disordered and positively charged N- and C-terminal regions. This is in strong agreement with the NMR-based solution structure of histone H1 containing a common structural motif of the four core histone proteins that consists of a long central α-helix with two adjacent smaller α-helices separated by loops (α1-L1-α2-L2-α3), with the remaining parts of this protein being highly disordered [111,112]. On the other hand, Fig. 6B illustrates that ProTα is completely disordered.

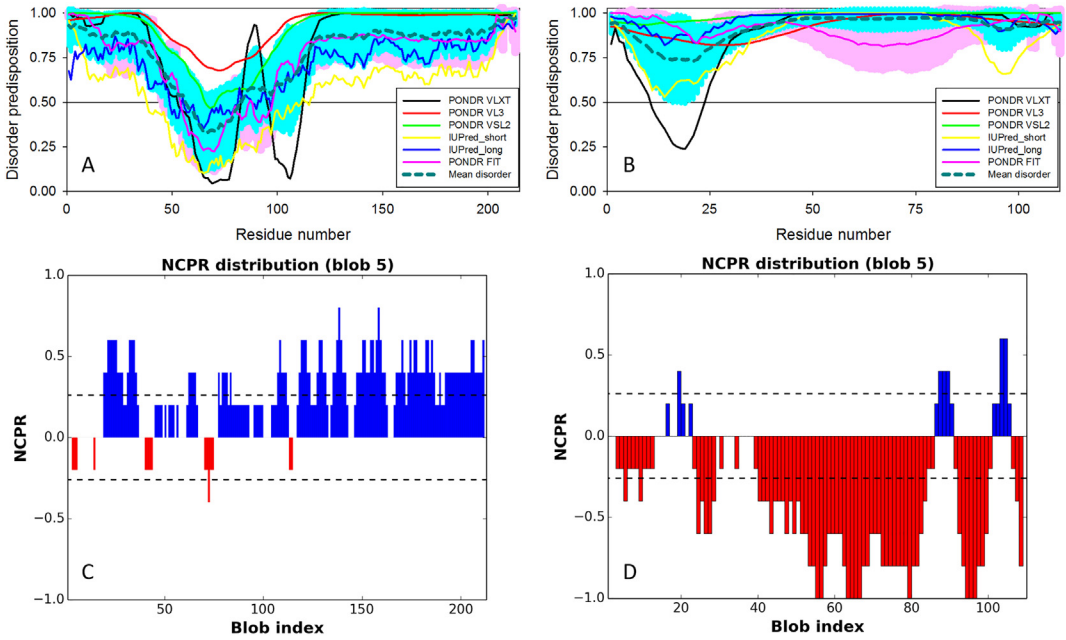


**Fig. 6.** Peculiarities of intrinsic disorder predisposition (panels A and B) and charge distribution (panels C and D) within the amino acid sequences of linker histone H1 (panels A and C) and ProTα (panels B and D). Intrinsic disorder propensities of the bovine linker histone H1 (UniProt ID: P02253) (A) bovine ProTα (UniProt ID: P01252) (B) were evaluated by PONDR® VLXT (black curves), PONDR® VL3 (red curves), PONDR® VSL2 (green curves), PONDR® FIT (pink curves), IUPred_short (yellow curves), and IUPred_long (blue curves). Mean disorder predisposition was calculated by averaging of all predictor-specific per-residue disorder profiles (bold, dashed, dark cyan curves). Light pink shadow around the PONDR® FIT curve represents error distribution for this predictor, whereas light blue shadow around the mean disorder curve show distribution of standard deviations. Peculiarities of the charge residues distribution within the amino acid sequences of the bovine linker histone H1 (UniProt ID: P02253) (C) bovine ProTα (UniProt ID: P01252) (D) were evaluated by CIDER and are shown as corresponding linear net charge per residue diagrams.

This conclusion is supported by the previous studies that clearly illustrated the highly disordered nature of this protein [107–109].

The presence of high levels of intrinsic disorder in these two proteins is expected, since both of them contain a large number of charged residues. In fact, there are 59 (27.7%), 4 (1.9%), 1 (0.5%), and 6 (2.8%) Lys, Arg, Asp, and Glu residues in histone H1, which gives this protein a mean net charge of +56. In addition to the presence of large number of charged residues, histone H1 contains high levels of major disorder-promoting residues [85,113,114], such as Ala (56, 26.3%), Pro (19, 8.9%), Ser (13, 6.1%), Thr (13, 6.1%), and Gly (13, 6.1%). Similarly, the mean net charge of ProTα is −43, since among 110 of its residues, there are 35 (31.8%), 18 (16.4%), 8 (7.3%), and 2 (1.8%) Glu, Asp, Lys, and Arg, respectively. Furthermore, this protein does not have major order-promoting residues, such as aromatic residues and cysteins, but contains many disorder-promoting residues, including Ala (12, 10.9%), Gly (9, 8.2%), Thr (6, 5.5%), and Ser (3, 2.7%). Therefore, based on the charge-hydropathy analysis, where proteins are classified as wholly disordered or wholly ordered/compact based on their absolute normalized mean net charge and mean hydrophobicity [115], both histone H1 and ProTα were predicted to be wholly disordered (see Figs. S3 and S4).

However, it was also pointed out that the analysis of the peculiarities of the distribution of positively and negatively charged residues within the amino acid sequence of a query protein can provide more specific characterization of its expected conformational behavior [96]. To this end, a computational platform CIDER (http://pappulab.wustl.edu/CIDER/analysis/) provides information on the fraction of charged residues (FCR) and extent of charged amino acid mixing in a sequence of a query protein (defined as parameter $\kappa$ that ranges from 1, where the charged residues are segregated into two blobs containing all positively or negatively charged residues, and 0, where the positively and negatively charged residues are evenly mixed throughout the sequence). Furthermore, CIDER shows the corresponding linear net charge per residue diagram and represents the Das-Pappu phase diagram which provides a means to estimating how a disordered sequence might behave based on the charge content [96]. Application of this tool revealed that histone H1 is characterized by an FCR of 0.329, an NCPR of +0.263, and a $\kappa$ of 0.204, whereas for ProTα, FCR, NCPR, and $\kappa$ are 0.573, −0.391, and 0.423, respectively. Therefore, based on the values of their $\kappa$ parameter, histone H1 and ProTα are characterized by rather different distribution of their charged residues, with the charged residues being rather evenly distributed within the histone H1 sequence, but being grouped in blocks within the ProTα sequence. This observation is further illustrated by Fig. 6C and D, where the linear net charge per residue diagrams are shown for these proteins. Finally, based on their positions within the Das-Pappu phase diagram, histone H1 can be classified as a weak polyampholyte/polyelectrolyte behaving as a globule or a tadpole, while ProTα is a negatively charged strong polyelectrolyte behaving as a swollen globule (see Figs. S3 and S4).

### *3.6. pH-induced conformational changes in the intrinsically disordered ProTα and linker histone H1 in the concentrated PEG solutions*

The results of measuring the pH-induced transitions in poly-E, poly-K, and poly-R can only remotely simulate the behavior of the majority of IDPs, since the lengths of the poly-K, poly-E, and poly-R peptides studied are significantly larger than the lengths of many poly-K, poly-E, and poly-R tracts observed in real IDPs. In addition, in IDPs (which are biological heteropolymers), charges can have different clustering. Furthermore, even in the presence of a large number of E or K residues, IDPs might contain a sufficiently large number of oppositely charged amino acids, so their total charge is low. Considering all this, we selected ProTα and histone H1 (whose amino acid sequences contain approximately 30% glutamic acid and lysine, respectively) as IDPs, with which the results obtained for polypeptides were compared.

It was established that the macromolecular crowding conditions contribute to the aggregation of histone H1 at almost the entire pH range under the all experimental conditions. The presence of aggregation was manifested by a significant decrease in the recorded far-UV CD signal in comparison with diluted solutions (Fig. 7). The formation of amorphous aggregates by proteins in macromolecular crowding

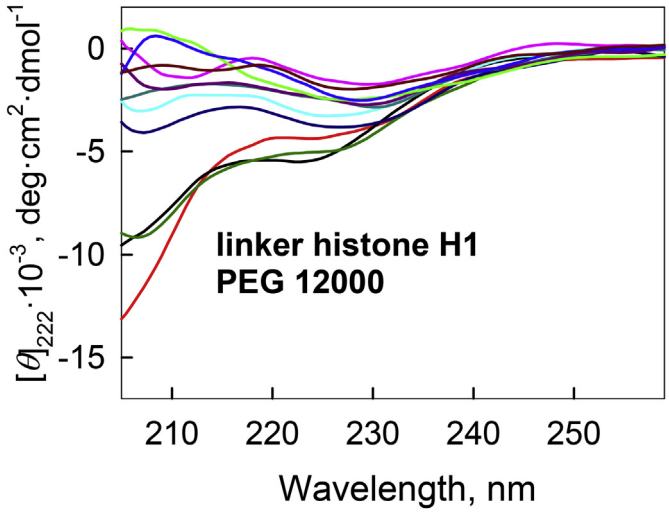


**Fig. 7.** Conformational changes of linker histone H1 induced by pH change in PEG 12,000 solutions. The far-UV CD spectra of histone H1 in PEG 12,000 solutions with pH 2.6, 4.3, 5.3, 6.2, 7.0, 8.0, 9.3, 9.9, 10.5, 11.0, and 11.8 are represented by black, red, green, blue, pink, cyan, dark red, dark green, dark blue, purple, and dark cyan curves, respectively.

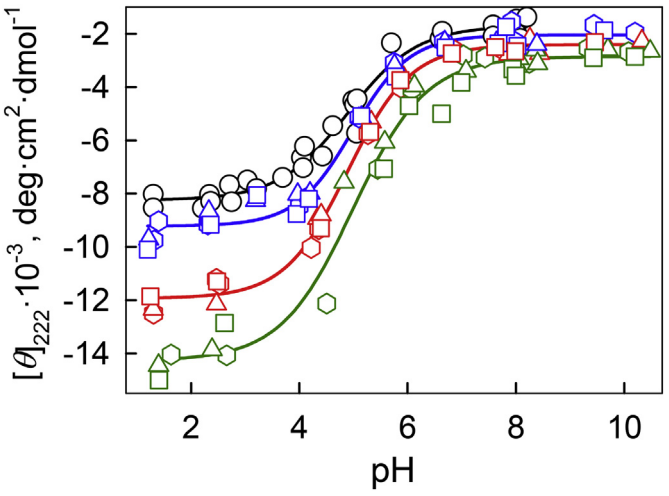


**Fig. 8.** pH-induced conformational changes in ProTα under the conditions of macromolecular crowding. The dependences of molar ellipticity at 222 nm of ProTα in PEG solutions with molecular weight of 600 Da (hexagons), 4000 Da (triangles) and 12,000 Da (squares) and with concentration of 0, 80, 200, and 300 mg/mL are represented by black, blue, green red curves, respectively.

conditions is a fairly common phenomenon associated with restriction of conformational heterogeneity of proteins [19]. As was mentioned above, histone H1 represents a hybrid protein containing a more ordered (and more hydrophobic) central region and highly disordered positively charged N- and C-tails. For example, the C-terminal domain (CTD) of this protein (~100 amino acids) is very basic, containing ~40% Lys residues, the majority of which (~75%) are present as doublets. In diluted solutions, this CTD has little structure but can cooperatively fold upon interaction with DNA [116–119]. Importantly, it was established that under macromolecular crowding conditions, noticeable compaction of the C-terminal domain of the histone H1 takes place, leading to the formation of a molten globule-like conformation [120].

Earlier, it was shown that in the diluted solutions, ProTα, which is highly disordered and expanded at neutral pH, is capable of adopting partially folded collapsed conformation at acidic pH [108]. When free volume is limited (i.e., in the presence of macromolecular crowders), the pH-induced conformational transitions of ProTα generally correspond to the structural transitions of poly-glutamic acid under comparable conditions, where an increase in the cooperativity of the transition caused by the deionization of the polypeptide chain is observed when the PEG size increases (Fig. 8). These data indicate the possibility of using poly-E conformational transitions to simulate conformational transitions of this protein.

Taken together, these results indicate that under the conditions of extreme macromolecular crowding, which is likely to correspond to the environment of IDPs in PMLOs, the conformational transitions of poly-amino acids and highly charged IDPs can become more pronounced and can be accompanied by protein aggregation.

### *3.7. The effect of overcrowding conditions on the capability of poly-K and poly-E to form amyloid fibrils*

Under certain conditions, several poly-amino acids, including poly-E and poly-K, were shown to undergo an α-helix to β-sheet transition and form amyloid fibrils [67,121,122]. It was also pointed out that the $3_{10}$-helix formation can represent an intermediate stage during such α-helix–β-sheet transition [123]. Analysis of the poly-E (Fig. S5) and poly-K far-UV CD spectra (Fig. S6) showed that poly-K in highly concentrated PEG solutions with neutral pH contains $3_{10}$-helix. Although energetically $3_{10}$-helix is less favorable than α-helical or β-structural conformation, it is known that increasing in the excluded volume can contribute to the stabilization of some high-energy conformations of polypeptide chain [31,33,51].

In order to determine the content of $3_{10}$-helices in the secondary structure of poly-K at neutral pH, we measured the IR spectra of this homopolypeptide at pH 7 in dilute solutions and in solutions containing PEG 12,000 Da at the concentration of 300 mg/mL. The IR spectra of poly-E were also measured under the same conditions. It should be noted that in dilute solutions, the coil–α-helix transition at pH 7 was not yet observed in poly-K, whereas in the highly concentrated PEG solutions, the transition between the disordered and structured forms of poly-K at pH 7 already started (see Figs. 2 and 3). The opposite pattern was observed for the poly-E, where the coil–α-helix transition was already observed in the dilute solutions at pH 7, whereas in the highly concentrated PEG solutions, the poly-E structure was dominated by disordered conformation (Fig. 2).

Analysis of the IR data showed that the content of $3_{10}$-helices in the secondary structure of poly-K under the conditions of macromolecular crowding at pH 7 practically did not change compared to dilute solutions, whereas there was a significant increase in the α-helical structure and decrease in the content of β-sheet and irregular structure (Table 1, Fig. 9). These observations are consistent with the far-UV CD data showing the beginning of the coil–α-helix transition at the macromolecular crowding conditions in this pH range (Fig. 2). In solutions containing poly-E at pH 7, the characteristic of $3_{10}$-helix absorption peak at $\nu = 1641\ cm^{-1}$ is not present under all conditions studied (both in the absence or presence of PEG). On the other hand, IR analysis revealed that the macromolecular crowding contributes to the decrease in the helical content of poly-E, paralleled with some increase in the β-structure

**Table 1**
The distribution of elements in the secondary structure of poly-K and poly-E according to the FTIR data at pH 7 (solvent is $D_2O$). Analysis was performed according to [81,82].

| PEG 12,000 | α-Helix, % | $3_{10}$-Helix, % | β-Sheet, % | β-Turn, % | Random, % |
|---|---|---|---|---|---|
| Poly-K | | | | | |
| 0 mg/ml | 21.1 | 25.3 | 24.9 | 28.7 | 0 |
| 300 mg/ml | 67.8 | 23.2 | 3.3 | 5.7 | 0 |
| Poly-E | | | | | |
| 0 mg/ml | 33.2 | 10.4 | 22.7 | 28.7 | 5 |
| 300 mg/ml | 23.9 | 0 | 34.2 | 23.8 | 18.1 |

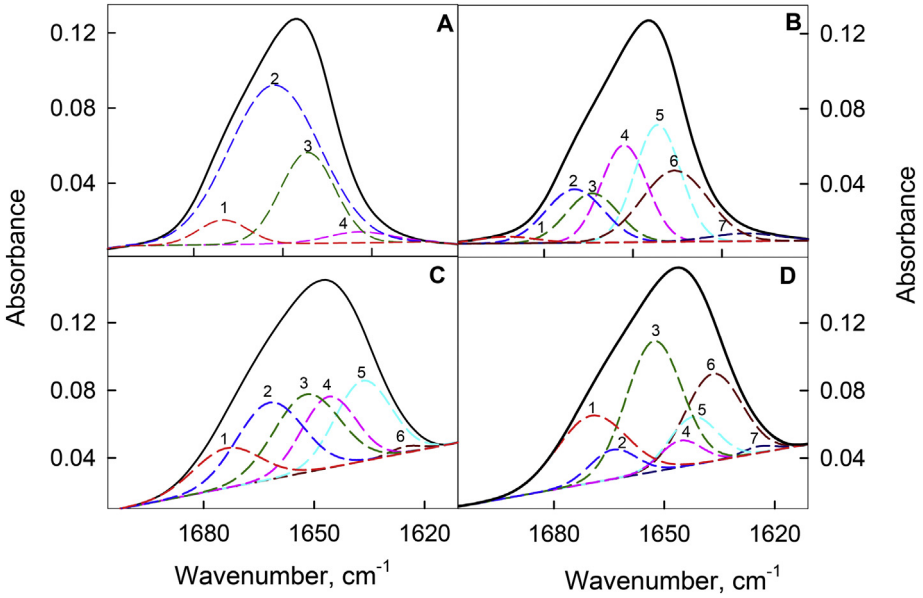


**Fig. 9.** Decomposition of the amide I′ FTIR absorption bands of poly-K and poly-E spectra. Amide I′ absorption bands of poly-E (panels A and C) poly-K (panels B and D) and are represented in solution without PEG (panels A and B) and in solution containing 300 mg/mL of PEG 12,000 (panels C and D) at pH 7. The polymerization degrees of poly-amino acids were 200 (for poly-E) and 250 (for poly-K).

content and significant increase in the proportion of disordered regions (Table 1, Fig. 9). These results are consistent with the far-UV CD data showing an increase in the cooperativity of coil–α-helix transition under the conditions of macromolecular crowding in comparison with this transition observed in the dilute solutions. As a result of this increase in cooperativity, the transition was not yet observed at pH 7 in the presence of high concentrations of PEG with high molecular weight (Fig. 2).

These data suggest that the conditions of macromolecular crowding do not contribute to the stabilization of $3_{10}$-helices in studied poly-amino acids, and apparently do not have a noticeable effect on the possible α-helix–β-sheet transition and the formation of amyloid fibrils by poly-K and poly-E at neutral pH.

Overall, out data suggest that the overcrowded conditions promote significant changes in the cooperativity of the pH-induced coil–α-helix transition of poly-E, poly-K, and ProTα and provoke histone H1 aggregation. We also show that in systems we studied, the most favorable conditions for the pH-induced structural transitions in the presence of high PEG concentrations can be reached when the charged residues are grouped in blocks, and when the distance between the end of the side group carrying charge and the backbone is small. Therefore, block-wise distribution of charged residues within the studied IDPs not only plays an important role in the liquid–liquid phase transitions, but also defines the expressivity of structural transitions of these proteins in the overcrowded conditions of the membrane-less organelles. However, it should be kept in mind that a number of IDPs with charge blocks show no significant conformational changes upon phase separation, which in and of itself is a very crowed environment. This conclusion is based on NMR studies of several IDPs undergoing liquid-liquid phase separation, such as elastin-like polypeptides (ELPs) derived from the tropoelastin [124], Alzheimer disease-related protein tau [18], and C-terminal low-complexity (LC) domain of the hnRNPA2 protein [125]. In fact, ELPs, in their pre-transition state, were shown to represent highly dynamic and disordered chains containing transient β-turns, and this high conformational disorder was retained after phase separation [124]. Similarly, tau protein was shown to stay largely disordered within liquid droplets [18], and the structure of the LC domain of hnRNPA2 remained predominantly disordered in the phase-separated state [125]. Therefore, at least for these proteins, phase separation, which represents a natural crowding event, did not induce global structural rearrangements.

## 4. Conclusions

Our study showed that pH-induced coil–α-helix transitions in the charged poly-amino acids such as poly-E and poly-K can be used as a model of the pH-induced transition in highly charged IDPs, such as ProTα and linker histone H1. The examination of the poly-E and poly-K coil–α-helix transitions in the presence of PEG as a crowding agent revealed that the capability of PEG to form hydrogen bonds must be taken into account alongside with excluding volume effect, since at alkaline pH, these two effect are summed up, whereas at the acidic pH, the action of these two factors is opposite.

The established trends make it possible to explain the increase in the cooperativity of the coil–α-helix transition of ProTα and the aggregation of linker histone H1 in the overcrowded milieu. In fact, glutamic acid residues in the amino acid sequence of ProTα are grouped into blocks. This contributes to the increase in the cooperativity of the coil–α-helix transition under the conditions of macromolecular crowding. On the other hand, the lysine residues are more evenly distributed within the histone H1 sequence, which can provoke protein aggregation at the overcrowded conditions. It is interesting to note that the longest blocks of lysine residues (3 residues each) are located within the C-terminal domain of histone H1, which is known to undergo noticeable ordering at the conditions of macromolecular crowding [120].

The distribution of oppositely charged residues in a polypeptide sequence determines the conformation of polyampholytes, which include many IDPs [17]. In this case, sequences containing extended blocks of charged residues are more prone for liquid–liquid phase transitions than sequences with a fairly uniform distribution of charged residues throughout their sequences [126]. The results of our study suggest that the block distribution of charged residues in the sequences of PMLO-located IDPs not only promotes liquid–liquid phase transitions, but may also lead to an increase in the cooperativity of structural transitions and to general compaction of the polypeptide chain in overcrowded conditions.

## Acknowledgements

We are thankful to Alexey Uversky for careful reading and editing of this manuscript. The work was supported in part by a grants from the President of the Russian Federation scholarship SP-3665.2018.4

(histone H1 study, AVF), Russian Science Foundation RSCF 18-75-10115 (studies of poly-amino acid conformational changes, AVF), and from the Russian Foundation for Basic Research RFBR 18-34-00975 (prothymosin alpha study, IAA) and RFBR 18-08-01500 (IR-studies, AMP).

## Appendix A. Supplementary data

Supplementary data to this article can be found online at https://doi.org/10.1016/j.ijbiomac.2018.12.038.

## References

[1] E.J. Cho, J.S. Kim, Crowding effects on the formation and maintenance of nuclear bodies: insights from molecular-dynamics simulations of simple spherical model particles, Biophys. J. 103 (3) (2012) 424–433.
[2] V.N. Uversky, I.M. Kuznetsova, K.K. Turoverov, B. Zaslavsky, Intrinsically disordered proteins as crucial constituents of cellular aqueous two phase systems and coacervates, FEBS Lett. 589 (1) (2015) 15–22.
[3] V.N. Uversky, Intrinsically disordered proteins in overcrowded milieu: membraneless organelles, phase separation, and intrinsic disorder, Curr. Opin. Struct. Biol. 44 (2016) 18–30.
[4] O. Bounedjah, L. Hamon, P. Savarin, B. Desforges, P.A. Curmi, D. Pastre, Macromolecular crowding regulates assembly of mRNA stress granules after osmotic stress: new role for compatible osmolytes, J. Biol. Chem. 287 (4) (2012) 2446–2458.
[5] L.P. Bergeron-Sandoval, N. Safaee, S.W. Michnick, Mechanisms and consequences of macromolecular phase separation, Cell 165 (5) (2016) 1067–1079.
[6] A.M. Rice, M.K. Rosen, ATP controls the crowd, Science 356 (6339) (2017) 701–702.
[7] S. Kroschwald, S. Maharana, D. Mateju, L. Malinovska, E. Nuske, I. Poser, D. Richter, S. Alberti, Promiscuous interactions and protein disaggregases determine the material state of stress-inducible RNP granules, eLife 4 (2015), e06807.
[8] Y. Shin, C.P. Brangwynne, Liquid phase condensation in cell physiology and disease, Science 357 (6357) (2017), eaaf4382.
[9] T.J. Nott, E. Petsalaki, P. Farber, D. Jervis, E. Fussner, A. Plochowietz, T.D. Craggs, D.P. Bazett-Jones, T. Pawson, J.D. Forman-Kay, A.J. Baldwin, Phase transition of a disordered nuage protein generates environmentally responsive membraneless organelles, Mol. Cell 57 (5) (2015) 936–947.
[10] D.M. Mitrea, R.W. Kriwacki, Phase separation in biology; functional organization of a higher order, Cell Commun. Signal. 14 (2016) 1.
[11] R. Hancock, Structures and functions in the crowded nucleus: new biophysical insights, Front. Phys. 2 (53) (2014).
[12] S. Elbaum-Garfinkle, Y. Kim, K. Szczepaniak, C.C. Chen, C.R. Eckmann, S. Myong, C.P. Brangwynne, The disordered P granule protein LAF-1 drives phase separation into droplets with tunable viscosity and dynamics, Proc. Natl. Acad. Sci. U. S. A. 112 (23) (2015) 7189–7194.
[13] S.F. Banani, H.O. Lee, A.A. Hyman, M.K. Rosen, Biomolecular condensates: organizers of cellular biochemistry, Nat. Rev. Mol. Cell Biol. 18 (5) (2017) 285–298.
[14] C.W. Pak, M. Kosno, A.S. Holehouse, S.B. Padrick, A. Mittal, R. Ali, A.A. Yunus, D.R. Liu, R.V. Pappu, M.K. Rosen, Sequence determinants of intracellular phase separation by complex coacervation of a disordered protein, Mol. Cell 63 (1) (2016) 72–85.
[15] Y.H. Lin, J.D. Forman-Kay, H.S. Chan, Sequence-specific polyampholyte phase separation in membraneless organelles, Phys. Rev. Lett. 117 (17) (2016), 178101.
[16] Y. Lin, D.S. Protter, M.K. Rosen, R. Parker, Formation and maturation of phase-separated liquid droplets by RNA-binding proteins, Mol. Cell 60 (2) (2015) 208–219.
[17] R.K. Das, R.V. Pappu, Conformations of intrinsically disordered proteins are influenced by linear sequence distributions of oppositely charged residues, Proc. Natl. Acad. Sci. U. S. A. 110 (33) (2013) 13392–13397.
[18] S. Ambadipudi, J. Biernat, D. Riedel, E. Mandelkow, M. Zweckstetter, Liquid-liquid phase separation of the microtubule-binding repeats of the Alzheimer-related protein Tau, Nat. Commun. 8 (1) (2017) 275.
[19] I.M. Kuznetsova, K.K. Turoverov, V.N. Uversky, What macromolecular crowding can do to a protein, Int. J. Mol. Sci. 15 (12) (2014) 23090–23140.
[20] X. Ai, Z. Zhou, Y. Bai, W.Y. Choy, $^{15}$N NMR spin relaxation dispersion study of the molecular crowding effects on protein folding under native conditions, J. Am. Chem. Soc. 128 (12) (2006) 3916–3917.
[21] X. Aguilar, F.W.C.T. Sparrman, M. Wolf-Watz, P. Wittung-Stafshede, Macromolecular crowding extended to a heptameric system: the co-chaperonin protein 10, Biochemistry 50 (14) (2011) 3034–3044.
[22] M.S. Cheung, D. Klimov, D. Thirumalai, Molecular crowding enhances native state stability and refolding rates of globular proteins, Proc. Natl. Acad. Sci. U. S. A. 102 (13) (2005) 4753–4758.
[23] M.S. Cheung, D. Thirumalai, Effects of crowding and confinement on the structures of the transition state ensemble in proteins, J. Phys. Chem. B 111 (28) (2007) 8250–8257.
[24] A. Christiansen, Q. Wang, M.S. Cheung, P. Wittung-Stafshede, Effects of macromolecular crowding agents on protein folding in vitro and in silico, Biophys. Rev. 5 (2) (2013) 137–145.
[25] A. Christiansen, Q. Wang, A. Samiotakis, M.S. Cheung, P. Wittung-Stafshede, Factors defining effects of macromolecular crowding on protein stability: an in vitro/in silico case study using cytochrome c, Biochemistry 49 (31) (2010) 6519–6530.
[26] A. Dhar, A. Samiotakis, S. Ebbinghaus, L. Nienhaus, D. Homouz, M. Gruebele, M.S. Cheung, Structure, function, and folding of phosphoglycerate kinase are strongly perturbed by macromolecular crowding, Proc. Natl. Acad. Sci. U. S. A. 107 (41) (2010) 17586–17591.
[27] A.V. Fonin, S.A. Silonov, A.K. Sitdikova, I.M. Kuznetsova, V.N. Uversky, K.K. Turoverov, Structure and conformational properties of D-glucose/D-galactose-binding protein in crowded milieu, Molecules 22 (2) (2017), E244.
[28] D. Homouz, M. Perham, A. Samiotakis, M.S. Cheung, P. Wittung-Stafshede, Crowded, cell-like environment induces shape changes in aspherical protein, Proc. Natl. Acad. Sci. U. S. A. 105 (33) (2008) 11754–11759.
[29] D. Homouz, H. Sanabria, M.N. Waxham, M.S. Cheung, Modulation of calmodulin plasticity by the effect of macromolecular crowding, J. Mol. Biol. 391 (5) (2009) 933–943.
[30] D. Homouz, L. Stagg, P. Wittung-Stafshede, M.S. Cheung, Macromolecular crowding modulates folding mechanism of alpha/beta protein apoflavodoxin, Biophys. J. 96 (2) (2009) 671–680.
[31] H. Kang, P.A. Pincus, C. Hyeon, D. Thirumalai, Effects of macromolecular crowding on the collapse of biopolymers, Phys. Rev. Lett. 114 (6) (2015), 068303.
[32] D.H. Kim, C. Lee, Y.J. Cho, S.H. Lee, E.J. Cha, J.E. Lim, T.M. Sabo, C. Griesinger, D. Lee, K.H. Han, A pre-structured helix in the intrinsically disordered 4EBP1, Mol. BioSyst. 11 (2) (2015) 366–369.
[33] A. Kudlay, M.S. Cheung, D. Thirumalai, Crowding effects on the structural transitions in a flexible helical homopolymer, Phys. Rev. Lett. 102 (11) (2009), 118101.
[34] B. Martínez-Haya, M.C. Gordillo, Effect of macromolecular crowding on the conformation of confined chain polymers, Macromol. Theory Simul. 14 (7) (2005) 421–427.
[35] T. Mikaelsson, J. Aden, P. Wittung-Stafshede, L.B. Johansson, Macromolecular crowding effects on two homologs of ribosomal protein s16: protein-dependent structural changes and local interactions, Biophys. J. 107 (2) (2014) 401–410.
[36] A. Samiotakis, M.S. Cheung, Folding dynamics of Trp-cage in the presence of chemical interference and macromolecular crowding. I, J. Chem. Phys. 135 (17) (2011), 175101.
[37] L. Stagg, S.Q. Zhang, M.S. Cheung, P. Wittung-Stafshede, Molecular crowding enhances native structure and stability of alpha/beta protein flavodoxin, Proc. Natl. Acad. Sci. U. S. A. 104 (48) (2007) 18976–18981.
[38] N. Tokuriki, M. Kinjo, S. Negi, M. Hoshino, Y. Goto, I. Urabe, T. Yomo, Protein folding by the effects of macromolecular crowding, Protein Sci. 13 (1) (2004) 125–133.
[39] B. van den Berg, R.J. Ellis, C.M. Dobson, Effects of macromolecular crowding on protein folding and aggregation, EMBO J. 18 (24) (1999) 6927–6933.
[40] Q. Wang, K.C. Liang, A. Czader, M.N. Waxham, M.S. Cheung, The effect of macromolecular crowding, ionic strength and calcium binding on calmodulin dynamics, PLoS Comput. Biol. 7 (7) (2011), e1002114.
[41] D.J. Winzor, P.R. Wills, Molecular crowding effects of linear polymers in protein solutions, Biophys. Chem. 119 (2) (2006) 186–195.
[42] J.M. Yuan, C.L. Chyan, H.X. Zhou, T.Y. Chung, H. Peng, G. Ping, G. Yang, The effects of macromolecular crowding on the mechanical stability of protein molecules, Protein Sci. 17 (12) (2008) 2156–2166.
[43] J.C. Bardwell, U. Jakob, Conditional disorder in chaperone action, Trends Biochem. Sci. 37 (12) (2012) 517–525.
[44] S. Qin, H.X. Zhou, Effects of macromolecular crowding on the conformational ensembles of disordered proteins, J. Phys. Chem. Lett. 4 (20) (2013).
[45] V.N. Uversky, Intrinsically disordered proteins and their environment: effects of strong denaturants, temperature, pH, counter ions, membranes, binding partners, osmolytes, and macromolecular crowding, Protein J. 28 (7–8) (2009) 305–325.
[46] J. Dogan, S. Gianni, P. Jemth, The binding mechanisms of intrinsically disordered proteins, Phys. Chem. Chem. Phys. 16 (14) (2014) 6323–6331.
[47] K.K. Turoverov, I.M. Kuznetsova, V.N. Uversky, The protein kingdom extended: ordered and intrinsically disordered proteins, their folding, supramolecular complex formation, and aggregation, Prog. Biophys. Mol. Biol. 102 (2–3) (2010) 73–84.
[48] J. Aden, P. Wittung-Stafshede, Folding of an unfolded protein by macromolecular crowding in vitro, Biochemistry 53 (14) (2014) 2271–2277.
[49] A. Soranno, I. Koenig, M.B. Borgia, H. Hofmann, F. Zosel, D. Nettels, B. Schuler, Single-molecule spectroscopy reveals polymer effects of disordered proteins in crowded environments, Proc. Natl. Acad. Sci. U. S. A. 111 (13) (2014) 4874–4879.
[50] J.M. Mouillon, S.K. Eriksson, P. Harryson, Mimicking the plant cell interior under water stress by macromolecular crowding: disordered dehydrin proteins are highly resistant to structural collapse, Plant Physiol. 148 (4) (2008) 1925–1937.
[51] A. Kudlay, M.S. Cheung, D. Thirumalai, Influence of the shape of crowding particles on the structural transitions in a polymer, J. Phys. Chem. B 116 (29) (2012) 8513–8522.
[52] A.C. Sotomayor-Perez, O. Subrini, A. Hessel, D. Ladant, A. Chenal, Molecular crowding stabilizes both the intrinsically disordered calcium-free state and the folded calcium-bound state of a repeat in toxin (RTX) protein, J. Am. Chem. Soc. 135 (32) (2013) 11929–11934.
[53] J. Hong, L.M. Gierasch, Macromolecular crowding remodels the energy landscape of a protein by favoring a more compact unfolded state, J. Am. Chem. Soc. 132 (30) (2010) 10445–10452.
[54] R. Engel, A.H. Westphal, D.H. Huberts, S.M. Nabuurs, S. Lindhoud, A.J. Visser, C.P. van Mierlo, Macromolecular crowding compacts unfolded apoflavodoxin and causes severe aggregation of the off-pathway intermediate during apoflavodoxin folding, J. Biol. Chem. 283 (41) (2008) 27383–27394.
[55] N.C. Shirai, M. Kikuchi, The interplay of intrinsic disorder and macromolecular crowding on alpha-synuclein fibril formation, J. Chem. Phys. 144 (5) (2016), 055101.
[56] F.X. Theillet, A. Binolfi, T. Frembgen-Kesner, K. Hingorani, M. Sarkar, C. Kyne, C. Li, P.B. Crowley, L. Gierasch, G.J. Pielak, A.H. Elcock, A. Gershenson, P. Selenko,

Physicochemical properties of cells and their effects on intrinsically disordered proteins (IDPs), Chem. Rev. 114 (13) (2014) 6661–6714.
[57] A.V. Fonin, A.L. Darling, I.M. Kuznetsova, K.K. Turoverov, V.N. Uversky, Intrinsically disordered proteins in crowded milieu: when chaos prevails within the cellular gumbo, Cell. Mol. Life Sci. 75 (21) (2018) 3907–3929.
[58] V.N. Uversky, Unusual biophysics of intrinsically disordered proteins, Biochim. Biophys. Acta 1834 (5) (2013) 932–951.
[59] A. Badasyan, Y. Mamasakhlisov, R. Podgornik, V.A. Parsegian, Solvent effects in the helix-coil transition model can explain the unusual biophysics of intrinsically disordered proteins, J. Chem. Phys. 143 (1) (2015), 014102.
[60] E.A. Cino, M. Karttunen, W.Y. Choy, Effects of molecular crowding on the dynamics of intrinsically disordered proteins, PLoS One 7 (11) (2012), e49876.
[61] B. Hammouda, D. Ho, S. Kline, SANS from poly(ethylene oxide)/water systems, Macromolecules 35 (22) (2002) 8578–8585.
[62] B. Hammouda, D.L. Ho, S. Kline, Insight into clustering in poly(ethylene oxide) solutions, Macromolecules 37 (18) (2004) 6932–6937.
[63] E.M. Saffer, M.A. Lackey, D.M. Griffin, S. Kishore, G.N. Tew, S.R. Bhatia, SANS study of highly resilient poly(ethylene glycol) hydrogels, Soft Matter 10 (12) (2014) 1905–1916.
[64] E.J. Spek, Y. Gong, N.R. Kallenbach, Intermolecular Interactions in .alpha. Helical oligo- and poly(L-glutamic acid) at acidic pH, J. Am. Chem. Soc. 117 (43) (1995) 10773–10774.
[65] Y.P. Myer, The pH-induced helix-coil transition of poly-L-lysine and poly-L-glutamic acid and the 238-mμ dichroic band, Macromolecules 2 (6) (1969) 624–628.
[66] N. Lotan, A. Berger, E. Katchalski, Conformation and conformational transitions of poly-amino acids in solution, Annu. Rev. Biochem. 41 (1972) 869–902.
[67] M. Fandrich, C.M. Dobson, The behaviour of polyamino acids reveals an inverse side chain effect in amyloid structure formation, EMBO J. 21 (21) (2002) 5682–5690.
[68] T.V. Barskaya, O.B. Ptitsyn, Thermodynamic parameters of helix-coil transition in polypeptide chains. II. Poly-L-lysine, Biopolymers 10 (11) (1971) 2181–2197.
[69] V.E. Bychkova, O.B. Ptitsyn, T.V. Barskaya, Thermodynamic parameters of helix-coil transition in polypeptide chains. I. Poly-(L-glutamic acid), Biopolymers 10 (11) (1971) 2161–2179.
[70] A.M. Polyanichko, E.V. Chikhirzhina, A.N. Skvortsov, E.I. Kostyleva, P. Colson, C. Houssier, V.I. Vorob'ev, The HMG1 ta(i)le, J. Biomol. Struct. Dyn. 19 (6) (2002) 1053–1062.
[71] A.M. Polyanichko, E.V. Chikhirzhina, V.V. Andrushchenko, V.I. Vorob'ev, H. Wieser, The effect of manganese(II) on the structure of DNA/HMGB1/H1 complexes: electronic and vibrational circular dichroism studies, Biopolymers 83 (2) (2006) 182–192.
[72] E.V. Chikhirzhina, A.M. Polianichko, A.N. Skvortsov, E.I. Kostyleva, C. Houssier, V.I. Vorob'ev, HMG1 domains: the victims of circumstance, Mol. Biol. 36 (3) (2002) 525–531.
[73] S. Yi, A. Brickenden, W.Y. Choy, A new protocol for high-yield purification of recombinant human prothymosin alpha expressed in *Escherichia coli* for NMR studies, Protein Expr. Purif. 57 (1) (2008) 1–8.
[74] N. Sreerama, R.W. Woody, Computation and analysis of protein circular dichroism spectra, Methods Enzymol. 383 (2004) 318–351.
[75] J.Y. Su, R.S. Hodges, C.M. Kay, Effect of chain length on the formation and stability of synthetic alpha-helical coiled coils, Biochemistry 33 (51) (1994) 15501–15510.
[76] Y.H. Chen, J.T. Yang, K.H. Chau, Determination of the helix and beta form of proteins in aqueous solution by circular dichroism, Biochemistry 13 (16) (1974) 3350–3359.
[77] B.H. Zimm, J.K. Bragg, Theory of the phase transition between helix and random coil in polypeptide chains, J. Chem. Phys. 31 (2) (1959) 526–535.
[78] J. Applequist, On the helix-coil equilibrium in polypeptides, J. Chem. Phys. 38 (4) (1963) 934–941.
[79] O.B. Ptitsyn, Thermodynamic parameters of helix-coil transitions in polypeptide chains, Pure Appl. Chem. 31 (1) (1972) 227–244.
[80] M. Nagasawa, A. Holtzer, The helix-coil transition in solutions of polyglutamic acid, J. Am. Chem. Soc. 86 (4) (1964) 538–543.
[81] A. Barth, Infrared spectroscopy of proteins, Biochim. Biophys. Acta 1767 (9) (2007) 1073–1101.
[82] H. Yang, S. Yang, J. Kong, A. Dong, S. Yu, Obtaining information about protein secondary structures in aqueous solution using Fourier transform IR spectroscopy, Nat. Protoc. 10 (3) (2015) 382–396.
[83] A.M. Polianichko, N.M. Romanov, T. Starkova, E.I. Kostyleva, E.V. Chikhirzhina, Analysis of the secondary structure of linker histone H1 based on IR absorption spectra, Tsitologiia 56 (4) (2014) 316–322.
[84] I. Belaya, E. Chikhirzhina, A. Polyanichko, Interaction of DDP with bovine serum albumin facilitates formation of the protein dimers, J. Mol. Struct. 1140 (2017) 148–153.
[85] P. Romero, Z. Obradovic, X. Li, E.C. Garner, C.J. Brown, A.K. Dunker, Sequence complexity of disordered protein, Proteins 42 (1) (2001) 38–48.
[86] K. Peng, P. Radivojac, S. Vucetic, A.K. Dunker, Z. Obradovic, Length-dependent prediction of protein intrinsic disorder, BMC Bioinf. 7 (2006) 208.
[87] Z. Obradovic, K. Peng, S. Vucetic, P. Radivojac, C.J. Brown, A.K. Dunker, Predicting intrinsic disorder from amino acid sequence, Proteins 53 (Suppl. 6) (2003) 566–572.
[88] B. Xue, R.L. Dunbrack, R.W. Williams, A.K. Dunker, V.N. Uversky, PONDR-FIT: a meta-predictor of intrinsically disordered amino acids, Biochim. Biophys. Acta 1804 (4) (2010) 996–1010.
[89] Z. Dosztanyi, V. Csizmok, P. Tompa, I. Simon, IUPred: web server for the prediction of intrinsically unstructured regions of proteins based on estimated energy content, Bioinformatics 21 (16) (2005) 3433–3434.
[90] Z. Dosztanyi, V. Csizmok, P. Tompa, I. Simon, The pairwise energy content estimated from amino acid composition discriminates between folded and intrinsically unstructured proteins, J. Mol. Biol. 347 (4) (2005) 827–839.
[91] S.E. Permyakov, A.A. Vologzhannikova, P.A. Khorn, M.P. Shevelyova, A.S. Kazakov, V.I. Emelyanenko, A.I. Denesyuk, K. Denessiouk, V.N. Uversky, E.A. Permyakov, Comprehensive analysis of the roles of 'black' and 'gray' clusters in structure and function of rat beta-parvalbumin, Cell Calcium 75 (2018) 64–78.
[92] E.I. Deryusheva, A.I. Denesyuk, K. Denessiouk, V.N. Uversky, S.E. Permyakov, E.A. Permyakov, On the relationship between the conserved 'black' and 'gray' structural clusters and intrinsic disorder in parvalbumins, Int. J. Biol. Macromol. 120 (Pt A) (2018) 1055–1062.
[93] I. Walsh, M. Giollo, T. Di Domenico, C. Ferrari, O. Zimmermann, S.C. Tosatto, Comprehensive large-scale assessment of intrinsic protein disorder, Bioinformatics 31 (2) (2015) 201–208.
[94] X. Fan, L. Kurgan, Accurate prediction of disorder in protein chains with a comprehensive and empirically designed consensus, J. Biomol. Struct. Dyn. 32 (3) (2014) 448–464.
[95] Z. Peng, L. Kurgan, On the complementarity of the consensus-based disorder prediction, Pacific Symposium on Biocomputing. Pacific Symposium on Biocomputing 2012, pp. 176–187.
[96] A.S. Holehouse, R.K. Das, J.N. Ahad, M.O. Richardson, R.V. Pappu, CIDER: resources to analyze sequence-ensemble relationships of intrinsically disordered proteins, Biophys. J. 112 (1) (2017) 16–21.
[97] A.V. Finkelstein, O.B. Ptitsyn, Protein Physics: A Course of Lectures: Second, Updated and extended edition, 2016.
[98] H.T. Tran, A. Mao, R.V. Pappu, Role of backbone-solvent interactions in determining conformational equilibria of intrinsically disordered proteins, J. Am. Chem. Soc. 130 (23) (2008) 7380–7392.
[99] D.A. Brant, Conformational energy estimates for helical polypeptide molecules, Macromolecules 1 (4) (1968) 291–300.
[100] Q. Xu, J. Mi, C. Zhong, Structure of poly(ethylene glycol)-water mixture studied by polymer reference interaction site model theory, J. Chem. Phys. 133 (17) (2010), 174104.
[101] J.B. Zhang, P.Y. Zhang, K. Ma, F. Han, G.H. Chen, X.H. Wei, Hydrogen bonding interactions between ethylene glycol and water: density, excess molar volume, and spectral study, Sci. China Ser. B 51 (5) (2008) 420–426.
[102] A. Koutsioubas, D. Lairez, S. Combet, G.C. Fadda, S. Longeville, G. Zalczer, Crowding effect on helix-coil transition: beyond entropic stabilization, J. Chem. Phys. 136 (21) (2012), 215101.
[103] P.E. Mason, G.W. Neilson, C.E. Dempsey, A.C. Barnes, J.M. Cruickshank, The hydration structure of guanidinium and thiocyanate ions: implications for protein stability in aqueous solution, Proc. Natl. Acad. Sci. U. S. A. 100 (8) (2003) 4557–4561.
[104] C.T. Armstrong, P.E. Mason, J.L. Anderson, C.E. Dempsey, Arginine side chain interactions and the role of arginine as a gating charge carrier in voltage sensitive ion channels, Sci. Rep. 6 (2016), 21759.
[105] D. Piovesan, F. Tabaro, I. Micetic, M. Necci, F. Quaglia, C.J. Oldfield, M.C. Aspromonte, N.E. Davey, R. Davidovic, Z. Dosztanyi, A. Elofsson, A. Gasparini, A. Hatos, A.V. Kajava, L. Kalmar, E. Leonardi, T. Lazar, S. Macedo-Ribeiro, M. Macossay-Castillo, A. Meszaros, G. Minervini, N. Murvai, J. Pujols, D.B. Roche, E. Salladini, E. Schad, A. Schramm, B. Szabo, A. Tantos, F. Tonello, K.D. Tsirigos, N. Veljkovic, S. Ventura, W. Vranken, P. Warholm, V.N. Uversky, A.K. Dunker, S. Longhi, P. Tompa, S.C. Tosatto, DisProt 7.0: a major update of the database of disordered proteins, Nucleic Acids Res. 45 (D1) (2017) D1123–d1124.
[106] M. Sickmeier, J.A. Hamilton, T. Legall, V. Vacic, M.S. Cortese, A. Tantos, B. Szabo, P. Tompa, J. Chen, V.N. Uversky, Z. Obradovic, A.K. Dunker, DisProt: the database of disordered proteins, Nucleic Acids Res. 35 (Database) (2007) D786–D793.
[107] V.N. Uversky, J.R. Gillespie, I.S. Millett, A.V. Khodyakova, R.N. Vasilenko, A.M. Vasiliev, I.L. Rodionov, G.D. Kozlovskaya, D.A. Dolgikh, A.L. Fink, S. Doniach, E.A. Permyakov, V.M. Abramov, $Zn^{2+}$-mediated structure formation and compaction of the "natively unfolded" human prothymosin alpha, Biochem. Biophys. Res. Commun. 267 (2) (2000) 663–668.
[108] V.N. Uversky, J.R. Gillespie, I.S. Millett, A.V. Khodyakova, A.M. Vasiliev, T.V. Chernovskaya, R.N. Vasilenko, G.D. Kozlovskaya, D.A. Dolgikh, A.L. Fink, S. Doniach, V.M. Abramov, Natively unfolded human prothymosin alpha adopts partially folded collapsed conformation at acidic pH, Biochemistry 38 (45) (1999) 15009–15016.
[109] K. Gast, H. Damaschun, K. Eckert, K. Schulze-Forster, H.R. Maurer, M. Muller-Frohne, D. Zirwer, J. Czarnecki, G. Damaschun, Prothymosin alpha: a biologically active protein with random coil conformation, Biochemistry 34 (40) (1995) 13211–13218.
[110] Z. Peng, M.J. Mizianty, B. Xue, L. Kurgan, V.N. Uversky, More than just tails: intrinsic disorder in histone proteins, Mol. BioSyst. 8 (7) (2012) 1886–1901.
[111] K. Luger, A.W. Mader, R.K. Richmond, D.F. Sargent, T.J. Richmond, Crystal structure of the nucleosome core particle at 2.8 A resolution, Nature 389 (6648) (1997) 251–260.
[112] G. Arents, R.W. Burlingame, B.C. Wang, W.E. Love, E.N. Moudrianakis, The nucleosomal core histone octamer at 3.1 A resolution: a tripartite protein assembly and a left-handed superhelix, Proc. Natl. Acad. Sci. U. S. A. 88 (22) (1991) 10148–10152.
[113] A.K. Dunker, J.D. Lawson, C.J. Brown, R.M. Williams, P. Romero, J.S. Oh, C.J. Oldfield, A.M. Campen, C.M. Ratliff, K.W. Hipps, J. Ausio, M.S. Nissen, R. Reeves, C. Kang, C.R. Kissinger, R.W. Bailey, M.D. Griswold, W. Chiu, E.C. Garner, Z. Obradovic, Intrinsically disordered protein, J. Mol. Graph. Model. 19 (1) (2001) 26–59.
[114] P. Radivojac, L.M. Iakoucheva, C.J. Oldfield, Z. Obradovic, V.N. Uversky, A.K. Dunker, Intrinsic disorder and functional proteomics, Biophys. J. 92 (5) (2007) 1439–1456.
[115] V.N. Uversky, J.R. Gillespie, A.L. Fink, Why are "natively unfolded" proteins unstructured under physiologic conditions? Proteins 41 (3) (2000) 415–427.

[116] A. Roque, I. Iloro, I. Ponte, J.L. Arrondo, P. Suau, DNA-induced secondary structure of the carboxyl-terminal domain of histone H1, J. Biol. Chem. 280 (37) (2005) 32141–32147.
[117] R. Vila, I. Ponte, M. Collado, J.L. Arrondo, P. Suau, Induction of secondary structure in a COOH-terminal peptide of histone H1 by interaction with the DNA: an infrared spectroscopy study, J. Biol. Chem. 276 (33) (2001) 30898–30903.
[118] A. Roque, I. Ponte, P. Suau, Role of charge neutralization in the folding of the carboxy-terminal domain of histone H1, J. Phys. Chem. B 113 (35) (2009) 12061–12066.
[119] X. Lu, J.C. Hansen, Revisiting the structure and functions of the linker histone C-terminal tail domain, Biochem. Cell Biol. 81 (3) (2003) 173–176.
[120] A. Roque, I. Ponte, P. Suau, Macromolecular crowding induces a molten globule state in the C-terminal domain of histone H1, Biophys. J. 93 (6) (2007) 2170–2177.
[121] K. Sankaranarayanan, N. Meenakshisundaram, Micro-viscosity induced conformational transitions in poly-L-lysine, RSC Adv. 6 (78) (2016) 74009–74017.
[122] A. Fulara, A. Lakhani, S. Wojcik, H. Nieznanska, T.A. Keiderling, W. Dzwolak, Spiral superstructures of amyloid-like fibrils of polyglutamic acid: an infrared absorption and vibrational circular dichroism study, J. Phys. Chem. B 115 (37) (2011) 11010–11016.
[123] Y. Singh, P.C. Sharpe, H.N. Hoang, A.J. Lucke, A.W. McDowall, S.P. Bottomley, D.P. Fairlie, Amyloid formation from an alpha-helix peptide bundle is seeded by 3 (10)-helix aggregates, Chemistry 17 (1) (2011) 151–160.
[124] S.E. Reichheld, L.D. Muiznieks, F.W. Keeley, S. Sharpe, Direct observation of structure and dynamics during phase separation of an elastomeric protein, Proc. Natl. Acad. Sci. U. S. A. 114 (22) (2017) E4408–E4415.
[125] V.H. Ryan, G.L. Dignon, G.H. Zerze, C.V. Chabata, R. Silva, A.E. Conicella, J. Amaya, K.A. Burke, J. Mittal, N.L. Fawzi, Mechanistic view of hnRNPA2 low-complexity domain structure, interactions, and phase separation altered by mutation and arginine methylation, Mol. Cell 69 (3) (2018) 465–479.e7.
[126] Y.H. Lin, H.S. Chan, Phase separation and single-chain compactness of charged disordered proteins are strongly correlated, Biophys. J. 112 (10) (2017) 2043–2046.